Supporting Information for: A Study of Through-Space and Through-Bond *J*(PP) Coupling in Rigid Non-Symmetrical Bis(phosphine) and its Metal Complexes

Brian A. Chalmers,[a] Phillip Nejman,[a] Alice V. Llewellyn,[a] Adrian M. Felaar,[a] Ben L. Griffiths,[a] Eden I. Portman,[a] Emma-Jane L. Gordon,[a] Kenny J. H. Fan,[a] J. D. Woollins,[a] M. Bühl,[a] Olga L. Malkina,[b] David B. Cordes,[a] Alexandra M. Z. Slawin,[a] Petr Kilian*[a]

[a]EaStChem School of Chemistry, University of St Andrews, St Andrews, Fife KY16 9ST, UK. Email: pk7@st-andrews.ac.uk

[b]Slovak Academy of Sciences, Institute of Inorganic Chemistry, SK-84536 Bratislava, Slovakia

Experimental

General Considerations

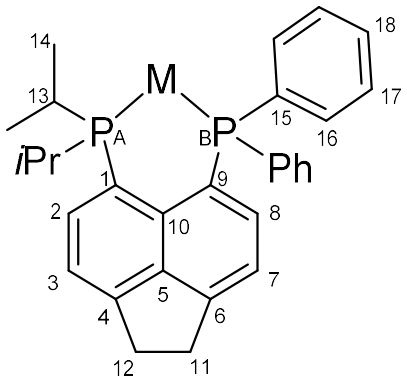

Figure S1: NMR Numbering scheme for all compounds

All reactions and manipulations were carried out under an atmosphere of oxygen free nitrogen using standard Schlenk techniques, or under an argon atmosphere in a Saffron glove box. Dry solvents were either collected from an MBraun Solvent Purification System, or dried and stored according to common procedures.[1] Other chemicals were purchased from Alfa Aesar, Sigma Aldrich or Strem Chemicals Ltd. and used as received. **L** and **[LPtCl$_2$]** were prepared according to the published

procedures.[2] All novel compounds were characterised by ^{1}H, $^{13}C\{^{1}H\}$ and $^{31}P\{^{1}H\}$ NMR, including measurement of $^{1}H\{^{31}P\}$, H-H DQF COSY, H-C HSQC, H-C HMBC and H-P HMBC where possible. ^{13}C NMR spectra were recorded using the DEPT-Q-135 pulse sequence with broadband proton decoupling. Measurements were performed at 25 °C using a JEOL GSX Delta 270 or Bruker Avance III 500 (MHz) spectrometer, unless otherwise specified. 85% H_3PO_4 was used as an external standard for ^{31}P NMR; ^{1}H and ^{13}C NMR shifts are relative to Me_4Si, residual solvent peaks were used for calibration ($CHCl_3$ δ_H 7.26, δ_C 77.2 ppm, CD_2Cl_2 δ_H 5.32, δ_C 53.8 ppm). Spin Simulations were performed using the WIN-DAISY application in TopSpin v3.5.[3] UV-vis spectra were acquired using a Shimadzu UV-1800 Spectrophotometer. Magnetic measurements were performed using a Johnson Matthey Magnetic Susceptibility Balance. Elemental analysis (C, H and N) was performed at London Metropolitan University. Mass Spectra were acquired in the EPSRC UK National Mass Spectrometry Facility (NMSF) at Swansea University. Infrared spectra were collected on a Perkin Elmer 2000 NIR FT spectrometer. "*In vacuo*" refers to a pressure of *ca.* 2×10^{-2} mbar.

Synthetic Procedures

[$LZnCl_2$]: To a suspension of **L** (295 mg, 0.66 mmol) in methanol (10 mL), a solution of zinc chloride (90 mg, 0.66 mmol) in methanol (10 mL) was added dropwise over 10 minutes. The solution was left to stir for 24 hours before the volatiles were removed *in vacuo* to afford **[$LZnCl_2$]** as an air-stable white solid (315 mg, 82%) (Mp. 286 °C, decomp.). Crystals of suitable quality for X-ray diffraction were grown from slow evaporation of solution of the complex in dichloromethane at ambient conditions. **Elemental Analysis:** Calcd. (%) for $C_{30}H_{32}P_2ZnCl_2{\cdot}½CH_2Cl_2$ (633.28): C 57.85, H 5.25; Found: C 57.92, H 5.44. **^{1}H NMR:** δ_H (500.1 MHz, $CDCl_3$) 7.77 (1H, dd ~t, $^{3}J_{HP} \approx {}^{3}J_{HH}$ = 7.7 Hz, H-2), 7.54–7.48 (5H, m, H-3,16), 7.48–7.45 (2H, m, H-18), 7.42–7.37 (4H, m, H-17), 7.36–7.32 (2H, m, H-7,8), 3.55–3.46 (4H, m, H-11,12), 2.44–2.33 (2H, m, H-13), 1.21 (6H, dd, $^{3}J_{HP}$ = 17.5, $^{3}J_{HH}$ = 6.9 Hz, 2 × CH_3, H-14), 0.99 (6H, dd, $^{3}J_{HP}$ = 15.5, $^{3}J_{HH}$ = 6.9 Hz, 2 × CH_3, H-14). **$^{13}C\{^{1}H\}$ NMR:** δ_C (125.8 MHz, $CDCl_3$) 152.6 (s, qC-6), 152.4 (s, qC-4), 140.9 (dd ~t, $^{3}J_{CP} \approx {}^{3}J_{CP}$ = 8.8 Hz, qC-5), 140.6 (s, C-8), 137.6 (s, C-2), 137.4 (dd ~t, $^{2}J_{CP} \approx {}^{2}J_{CP}$ = 14.3 Hz, qC-5), 134.5 (d, $^{2}J_{CP}$ = 13.3 Hz, C-16), 131.1 (s, C-18), 129.1 (d, $^{3}J_{CP}$ = 9.8 Hz, C-17), 128.5 (dd, $^{1}J_{CP}$ = 31.9, $^{5}J_{CP}$ = 5.3 Hz, qC-15), 120.5 (d, $^{3}J_{CP}$ = 6.1 Hz, C-7), 120.3 (m, qC-9), 120.2 (m, qC-1), 120.1 (d, $^{3}J_{CP}$ = 5.5 Hz, C-3), 30.3 (s, C-11/12), 30.0 (s, C-11/12), 26.1 (dd, $^{1}J_{CP}$ = 14.2, $^{5}J_{CP}$ = 4.3 Hz, C-13), 18.6 (d, $^{2}J_{CP}$ = 7.0 Hz, 2 × CH_3, C-14), 18.5 (d, $^{2}J_{CP}$ = 1.7 Hz, 2 × CH_3, C-14). **$^{31}P\{^{1}H\}$ NMR:** δ_P (202.5 MHz, $CDCl_3$) –3.1 (d, $^{2}J_{PP}$ = 193.0 Hz, P_A), –16.9 (d, $^{2}J_{PP}$ = 193.0 Hz, P_B). **HRMS (ASAP+):** m/z (%) calcd. for $C_{30}H_{32}P_2ZnCl$ 553.0959, found 553.0962 (20) [M–Cl]; m/z (%) calcd. for $C_{30}H_{33}P_2$ 455.2057, found 455.2029 (100)

[M–$ZnCl_2$]. **IR:** (KBr disc, cm^{-1}) ν = 3048w (ν_{Ar-H}), 2925m (ν_{C-H}), 1607s, 1437vs, 1312s, 1096s, 850s, 764s, 692vs, 549s.

[$LCdCl_2$]: To a suspension of **L** (145 mg, 0.32 mmol) in methanol (10 mL), a solution of $CdCl_2 \cdot 2.5H_2O$ (73 mg, 0.32 mmol) in methanol (10 mL) was added dropwise over 10 minutes. The solution was left to stir for 24 hours before the volatiles were removed *in vacuo* to afford **[$LCdCl_2$]** as an air-stable white solid (173 mg, 85%) (Mp. 275 °C decomp.). Crystals of suitable quality for X-ray diffraction were grown from slow evaporation of a solution of the complex in dichloromethane at ambient conditions. **Elemental Analysis:** Calcd. (%) for $C_{30}H_{32}P_2CdCl_2$ (637.84): C 56.50, H 5.06; Found: C 56.53, H 5.13. **^{1}H NMR:** δ_H (500.1 MHz, $CDCl_3$) 7.78 (1H, dd ~t, $^3J_{HH} \approx {}^3J_{HP}$ = 7.5 Hz, H-2), 7.48 (1H, d, $^3J_{HH}$ = 7.5 Hz, H-3), 7.47–7.44 (2H, m, H-18), 7.41–7.37 (8H, m, H-16,17), 7.32–7.29 (2H, m, H-3,7), 3.54–3.45 (4H, m, H-11,12), 2.43–2.32 (2H, m, H-13), 1.22 (6H, dd, $^3J_{HP}$ = 18.6, $^3J_{HH}$ = 6.9 Hz, 2 × CH_3, H-14), 0.84 (6H, dd, $^3J_{HP}$ = 16.2, $^3J_{HH}$ = 6.9 Hz, 2 × CH_3, H-14). **^{13}C{^{1}H} NMR:** δ_C (125.8 MHz, $CDCl_3$) 152.7 (s, qC-4), 152.6 (s, qC-6), 141.0 (dd ~t, $^3J_{CP}$ = 8.7 Hz, qC-5), 140.5 (d, $^2J_{CP}$ = 1.6 Hz, C-8), 137.8 (s, $^3J_{C\text{-}Cd}$ = 16.4 Hz, C-2), 137.3 (dd ~t, $^2J_{CP}$ = 14.5 Hz, qC-10), 134.5 (d, $^2J_{CP}$ = 15.2 Hz, C-16), 131.3 (s, C-18), 129.4 (d, $^3J_{CP}$ = 10.1 Hz, C-17), 128.6 (dd, $^1J_{CP}$ = 28.1, $^5J_{CP}$ = 4.9 Hz, qC-15), 121.3 (m, qC-9), 121.1 (m, qC-1), 120.5 (d, $^3J_{CP}$ = 6.0 Hz, C-7), 120.2 (d, $^3J_{CP}$ = 4.8 Hz, C-3), 30.3 (s, C-11/12), 30.0 (s, C-11/12), 26.9 (dd, $^1J_{CP}$ = 11.0, $^5J_{CP}$ = 4.0 Hz, C-13), 19.3 (d, $^2J_{CP}$ = 9.7 Hz, 2 × CH_3, C-14), 18.7 (d, $^2J_{CP}$ = 3.4 Hz, 2 × CH_3, H-14). **^{31}P{^{1}H} NMR:** δ_P (202.5 MHz, $CDCl_3$) 13.2 (d, $^2J_{PP}$ = 231.1 Hz, $^3J(^{31}P,^{113}Cd)$ = 1156.7, $^1J(^{31}P,^{111}Cd)$ = 1103.0 Hz, P_A), –6.6 (d, $^2J_{PP}$ = 231.1 Hz, $^3J(^{31}P,^{113}Cd)$ = 1025.0, $^1J(^{31}P,^{111}Cd)$ = 979.5 Hz, P_B). **HRMS (NSI+):** m/z (%) calcd. for $C_{30}H_{32}P_2CdOCl$ 619.0645, found 619.0635 (<1) [M+]; m/z (%) calcd. for $C_{30}H_{33}P_2$ 471.2007, found 471.1993 (100) [M–$CdCl_2$+H]. **IR:** (KBr disc, cm^{-1}) ν = 3050w (ν_{Ar-H}), 2961m (ν_{C-H}), 1607vs, 1435vs, 1313vs, 848vs, 765s, 748vs, 694vs, 619s.

[$LHgCl_2$]: To a solution of mercury(II) chloride (150 mg, 550 µmol) in ethanol (8 mL), a solution of **L** (250 mg, 550 µmol) in ethanol (20 mL) was added dropwise. The solution was left to stir for 2 hours. The volatiles were removed *in vacuo* to give **[$LHgCl_2$]** as an air-stable white solid (Mp. 234 °C decomp.) (395 mg, 99%). Crystals of suitable quality for X-ray diffraction were grown from slow evaporation of a solution of the complex in dichloromethane at ambient conditions. **Elemental Analysis**: Calcd. (%) for $C_{30}H_{32}P_2Cl_2Hg$) (726.02): C49.63, H 4.44. Found: C 49.55, H.4.41. **^{1}H NMR:** δ_H (500.1 MHz, CD_2Cl_2) 7.88 (1H, dd, $^4J_{HHg}$ = 28.3, $^3J_{HP}$ = 9.5, $^3J_{HH}$ = 7.3 Hz, H-2), 7.59 (1H, d, $^3J_{HH}$ = 7.3 Hz, H-3), 7.56–7.53 (2H, m, H-18), 7.49–7.41 (10H, m, H-7,8,16,17), 3.54 (4H, br s, H-11,12), 2.71 (2H, dh, $^3J_{HHg}$ = 81.7, $^2J_{HP}$ = 9.0, $^3J_{HH}$ = 6.8 Hz, H-13), 1.26 (6H, dd, $^3J_{HP}$ = 20.3, $^3J_{HH}$ = 6.8 Hz, 2 × CH_3, H-14), 0.87 (6H, dd, $^3J_{HP}$ = 17.3, $^3J_{HH}$ = 7.0 Hz, 2 × CH_3, H-14). **^{13}C{^{1}H} NMR:** δ_C (125.8 MHz, CD_2Cl_2) 154.2 (s, qC-4), 153.8 (s, qC-6), 141.2 (s,

qC-5), 140.8 (d, $^{3}J_{CHg}$ = 28.4, $^{2}J_{CP}$ = 2.6 Hz, C-8), 138.5 (s, $^{3}J_{HHg}$ = 63.9 Hz, C-2), 136.6 (dd, ~t, $^{2}J_{CP}$ = 12.9 Hz, qC-10), 134.4 (d, $^{2}J_{CP}$ = 14.8 Hz, C-16), 131.7 (d, $^{4}J_{CP}$ = 2.3 Hz, C-18), 129.4 (d, $^{3}J_{CP}$ = 10.8 Hz, C-17), 128.9 (dd, $^{1}J_{CP}$ = 32.6, $^{5}J_{CP}$ = 5.9 Hz, qC-15), 121.0 (d, $^{1}J_{CP}$ = 5.4 Hz, qC-9), 120.7 (d, $^{3}J_{CP}$ = 6.9 Hz, C-7), 120.5 (d, $^{3}J_{CP}$ = 6.4 Hz, C-3), 119.6 (dd, $^{1}J_{CP}$ = 23.5, $^{3}J_{CP}$ = 5.4 Hz, qC-1), 30.4 (s, C-11/12), 30.1 (s, C-11/12), 28.1 (dd, $^{1}J_{CP}$ = 14.8, $^{3}J_{CP}$ = 5.5 Hz, C-13), 18.6 (d, $^{3}J_{CHg}$ = 13.9, $^{2}J_{CP}$ = 8.3 Hz, 2 × CH_3, C-14), 17.8 (s, $^{3}J_{CHg}$ = 13.4 Hz, 2 × CH_3, C-14). **$^{31}P\{^{1}H\}$ NMR:** δ_P (202.5 MHz, CD_2Cl_2) 47.7 (d, $^{1}J_{PHg}$ = 3655.1, $^{2}J_{PP}$ = 309.0 Hz, P_A), 19.7 (d, $^{1}J_{PHg}$ = 2336.9 $^{2}J_{PP}$ = 309.0 Hz, P_B). **HRMS** (NSI+): *m/z* (%) Calcd. for $C_{30}H_{32}P_2ClHg$: 691.1363, found 691.1349 (100) [M–Cl]; Calcd. for $C_{60}H_{64}P_4Cl_3Hg_2$: 1417.2411, found 1417.2389 (25) [2M–Cl]. **IR:** (KBr disc, cm^{-1}) ν = 3050m ($\nu_{Ar–H}$), 2927m ($\nu_{C–H}$), 1608s, 1436vs, 1311s, 849s, 749s, 694s, 469m.

[$LNiCl_2$]: A yellow solution of **L** (210 mg, 0.46 mmol) in dichloromethane (10 mL), was added dropwise over 2 minutes to a green solution of nickel chloride hexahydrate (110 mg, 0.46 mmol) in methanol (5 mL). During addition, the solution turned an intense red colour. The solution was left to stir for 2 hours before the volatiles were removed *in vacuo* to afford **[$LNiCl_2$]** as an air-stable red solid (261 mg, 97%) (Mp. 140 °C decomp.). Crystals of suitable quality for X-ray diffraction were grown from slow evaporation of a solution of the complex in dichloromethane at ambient conditions. **Elemental Analysis:** Calcd. (%) for $C_{30}H_{32}P_2NiCl_2{\cdot}CH_2Cl_2$ (669.05): C 55.65, H 5.12; Found: C 55.75, H 5.20. **^{1}H NMR:** δ_H (500.1 MHz, $CDCl_3$, 298 K), 7.83 (1H, d, $^{3}J_{HH}$ = 7.4 Hz, H-2), 7.66–7.61 (4H, m, H-16), 7.48 (1H, d, $^{3}J_{HH}$ = 7.4 Hz, H-3), 7.44–7.37 (6H, m, H-17,18), 7.30–7.26 (1H, m, H-7), 7.10 (d, $^{3}J_{HH}$ = 7.4 Hz, H-8), 3.71 (2H, br s, H-13), 3.58–3.48 (4H, m, H-11,12), 1.40 (6H, d, $^{3}J_{HH}$ = 6.9 Hz, 2 × CH_3, H-14), 1.17 (6H, d, $^{3}J_{HH}$ = 6.9 Hz, 2 × CH_3, H-14). At lower temperatures, broadening of the lines due to the inhomogeneous nature of the sample precluded acquisition of high quality ^{1}H NMR spectrum with derivable coupling constants. **$^{13}C\{^{1}H\}$ NMR:** δ_C (125.8 MHz, $CDCl_3$, 298 K) 152.2 (s, qC-4), 151.9 (s, qC-6), 139.5 (s, C-8), 139.3 (s, qC-5), 137.3 (s, qC-10), 135.4 (s, C-2), 134.5 (s, C-16), 131.7 (s, qC-15), 131.0 (s, C-18), 128.4 (s, C-17), 120.0 (s, C-7), 119.1 (s, C-3), 116.5 (s, qC-9), 113.1 (s, qC-1), 30.4 (s, C-11/12), 30.3 (s, C-11/12), 29.2 (s, C-13), 20.7 (s, 2 × CH_3, C-14), 18.6 (s, 2 × CH_3, C-14). **$^{31}P\{^{1}H\}$ NMR:** δ_P (202.5 MHz, $CDCl_3$, 298 K) no signals observed. **$^{31}P\{^{1}H\}$ NMR:** δ_P (109.4 MHz, CD_2Cl_2, 193 K) 27.1 (d, $^{2}J_{PP}$ = 116.6 Hz, P_A), 14.3 (d, $^{2}J_{PP}$ = 116.6 Hz, P_B). **HRMS (ASAP+):** m/z (%) calcd. for $C_{30}H_{32}P_2NiCl_2$ 584.0679, found 584.0693 (<1) [M+]; m/z (%) calcd. for $C_{30}H_{32}P_2NiCl$ 547.1021, found 547.1022 (100) [M–Cl]; calcd. for $C_{30}H_{33}P_2O$ 471.2007, found 471.2006 (65) [M–$NiCl_2$+OH]. **UV-Vis:** λ_{MAX} (CH_2Cl_2)/nm 473 ($\varepsilon/M^{-1}cm^{-1}$ 455). **IR:** (KBr disc, cm^{-1}) ν = 3053w ($\nu_{Ar–H}$), 2952m ($\nu_{C–H}$), 1602s, 1434vs, 1317s, 1246s, 846s, 696vs, 591s.

[$LPdBr_2$]: To a suspension of dibromo(1,5-cyclooctadiene)palladium(II) (42 mg, 110 μmol) in dichloromethane (6 mL), a solution of **L** (51 mg, 110 μmol) in dichloromethane (10 mL) was added

dropwise. The solution was left to stir at room temperature for two hours. The volatiles were removed *in vacuo* to give **[LPdBr$_2$]** as an air-stable pale yellow solid (80 mg, 99%). Crystals of suitable quality for X-ray diffraction were grown from diffusion of hexane into a saturated solution of the complex in chloroform at ambient conditions. **Elemental Analysis:** Calcd. (%) for $C_{30}H_{32}P_2PdBr_2$·MeCN (862.58): C 44.56, H 4.09; Found: C 44.71, H 4.02. **^{1}H NMR:** δ_H (500.1 MHz, CD_2Cl_2) 7.96 (1H, dd ~t, $^3J_{HP} \approx {}^3J_{HH}$ = 7.2 Hz, H-2), 7.55 (1H, d, $^3J_{HH}$ = 7.2 Hz, H-3), 7.53–7.46 (6H, m, H-16,18), 7.43–7.38 (4H, m, H-18), 7.34 (1H, d, $^3J_{HH}$ = 7.4 Hz, H-7), 7.18 (1H, dd, $^3J_{HP}$ = 12.4, $^3J_{HH}$ = 7.4 Hz, H-8), 3.62–3.49 (6H, m, H-11,12,13), 1.27 (6H, dd, $^3J_{HP}$ = 18.8, $^3J_{HH}$ = 7.0 Hz, 2 × CH_3, H-14), 0.99 (6H, dd, $^3J_{HP}$ = 16.3, $^3J_{HH}$ = 7.0 Hz, 2 × CH_3, H-14). Note: qC atoms denoted with an asterisk (*) were not observed in the DEPTQ spectrum due to low solubility. These were however inferred *via* the H-C HMBC spectrum. **^{13}C{^{1}H} NMR:** δ_C (125.8 MHz, CD_2Cl_2) 153.4 (s, qC-4), 153.0 (s, qC-6), 139.5 (qC-5*), 139.3 (s, C-8), 137.5 (qC-10*), 135.1 (s, C-2), 134.2 (d, $^2J_{CP}$ = 11.0 Hz, C-16), 131.2 (s, C-18), 131.1 (qC-15*), 128.3 (d, $^3J_{CP}$ = 11.9 Hz, C-17), 119.9 (d, $^3J_{CP}$ = 9.4 Hz, C-7), 119.1 (d, $^3J_{CP}$ = 7.7 Hz, C-3), 114.5 (qC-9*), 112.0 (qC-1*), 30.4 (s, C-11/12), 30.3 (s, C-11/12), 30.2 (s, C-13), 19.9 (s, 2 × CH_3, C-14), 18.3 (s, 2 × CH_3, C-14). **^{31}P{^{1}H} NMR:** δ_P (202.5 MHz, CD_2Cl_2) 35.1 (d, $^2J_{PP}$ = 16.0 Hz, P_A), 18.5 (d, $^2J_{PP}$ = 16.0 Hz, P_B). **HRMS (ASAP+)**: *m/z* (%); Calcd. for $C_{30}H_{32}P_2PdBr$: 641.0196, found 641.0193 (100) [M–Br]. **IR:** (KBr disc, cm^{-1}) ν = 3048w (ν_{Ar-H}), 2955m (ν_{C-H}), 1598s, 1262s, 1093s, 850s, 744s, 692vs, 593vs.

[(LCuCl)$_2$]: To a suspension of cuprous chloride (33 mg, 330 μmol) in dichloromethane (6 mL), a solution of **L** (150 mg, 330 μmol) in dichloromethane (10 mL) was added dropwise. The solution was left to stir at room temperature overnight. The volatiles were removed *in vacuo* to give **[(LCuCl)$_2$]** as a mildly air-sensitive yellow solid (Mp. 248 °C decomp.) (178 mg, 98%). Crystals suitable for X-ray diffraction were grown *via* slow evaporation of a saturated solution of the complex in chloroform. **Elemental Analysis:** Calcd. (%) for $C_{60}H_{64}P_4Cl_2Cu_2$ (1107.04): C 65.10, H 5.83; Found: C 64.99, H 5.74. **^{1}H NMR:** δ_H (500.1 MHz, $CDCl_3$) 7.78–7.71 (2H, m), 7.46–7.26 (26H, m ~ br s), 3.46 (8H, br s, CH_2), 2.23 (4H, s, 2 × *i*Pr-CH), 1.19 (12H, br s, 4 × CH_3), 0.78 (12H, br s, 4 × CH_3). ^{13}C NMR could not be acquired due to low solubility and dynamic behavior in solution. **^{31}P{^{1}H} NMR:** δ_P (202.5 MHz, $CDCl_3$) 1.7 (d, $^2J_{PP}$ = 215.1 Hz, P_A), –14.8 (d, $^2J_{PP}$ = 216.0 Hz, P_B). **HRMS (ASAP+)**: *m/z* (%); Calcd. for $C_{60}H_{64}P_4Cu_2Cl$: 1071.2231, found 1071.2224 (100) [M–Cl]. **IR:** (KBr disc, cm^{-1}) ν = 3048w (ν_{Ar-H}), 2924m (ν_{C-H}), 1434s, 1314s, 845s, 745vs, 548m.

[L$_2$Ag]SbF$_6$: To a suspension of **L** (200 mg, 0.44 mmol) in methanol (10 mL), a solution of silver hexafluoroantimonate (75 mg, 0.22 mmol) in methanol (10 mL) was added dropwise over 2 minutes. The solution was left to stir for 1 hour before being filtered through a pad of celite. The volatiles were

removed *in vacuo* to afford **[L_2Ag]SbF_6** as an air-stable, light-sensitive, pale yellow solid (233 mg, 85%) (Mp. 155 °C decomp.). Crystals suitable for X-ray diffraction were grown *via* slow evaporation of a saturated solution of the complex in methanol. **Elemental Analysis:** Calcd. (%) for $C_{60}H_{64}P_4AgSbF_6$ (1252.66): C 57.53, H 5.15; Found: C 57.51, H 5.24. **^{1}H NMR:** δ_H (500.1 MHz, CD_2Cl_2) 7.81 (2H, dd ~t, $^3J_{HP} \approx {}^3J_{HH}$ = 7.2 Hz, H-2), 7.53 (2H, d, $^3J_{HH}$ = 7.2 Hz, H-3), 7.42–7.31 (10H, m, H-7,8,20,22), 7.26 (2H, tt, $^3J_{HH}$ = 7.4, $^4J_{HH}$ = 1.3 Hz, H-26), 7.19–7.15 (4H, m ~t, $^3J_{HH}$ = 7.8 Hz, H-21), 6.98–6.93 (4H, m ~t, $^3J_{HH}$ = 7.4 Hz, H-25), 6.70–6.65 (4H, m ~t, $^3J_{HP}$ = 8.8 Hz, H-24), 3.59–3.49 (8H, m, H-11,12), 2.33–2.34 (2H, m, H-16), 1.88–1.76 (2H, m, H-13), 1.01 (6H, dd, $^3J_{HP}$ = 15.5, $^3J_{HH}$ = 6.9 Hz, 2 × CH_3, H-17), 0.86 (6H, dd, $^3J_{HP}$ = 15.7, $^3J_{HH}$ = 6.9 Hz, 2 × CH_3, H-18), 0.82–0.74 (12H, m, 4 × CH_3, H-14,15). **^{13}C{^{1}H} NMR:** δ_C (125.8 MHz, CD_2Cl_2) 152.3 (s, qC-6), 151.5 (s, qC-4), 141.3–141.1 (m, qC-5), 140.5 (s, C-8), 137.8–137.6 (m, qC-10), 136.3 (qC-1*), 136.2 (s, C-2), 135.9–135.7 (m, qC-19), 134.7–134.5 (m, C-20), 132.8–132.6 (m, qC-23), 132.6–132.4 (m, C-24), 130.3 (s, C-22), 129.5 (s, C-26), 128.7 (s, C-21), 128.6 (s, C-25), 120.0 (s, C-7), 119.7 (s, C-3), 30.1 (s, C-11/12), 30.0 (s, C-11/12), 25.6 (br s, C-13,16), 22.0–21.8 (m, 2 × CH_3, C-15), 20.3–20.2 (m, 2 × CH_3, C-18), 19.1–18.9 (m, 2 × CH_3, C-17), 16.9 (br s, 2 × CH_3, C-14). **^{31}P{^{1}H} NMR:** δ_P (109.4 MHz, CD_2Cl_2) AA'MM'XX' spin system (A/A' = *i*Pr_2P; M/M' = Ph_2P; X = ^{107}Ag; X' = ^{109}Ag) δ_P 20.51 (m, A/A'), 0.67 (m, M/M'). $^2J_{AM} = {}^2J_{A'M'}$ = 171.5 Hz, $^2J_{AA'}$ = 17.2 Hz, $^2J_{MM'}$ = 16.3 Hz, $^2J_{AM'} = {}^2J_{A'M}$ = 0.9 Hz, $^1J_{AX}$ = 249.1 Hz, $^1J_{AX'}$ = 287.5 Hz, $^1J_{MX}$ = 172.9 Hz, $^1J_{MX'}$ = 200.6 Hz. **HRMS (NSI+):** m/z (%) calcd. for $C_{60}H_{64}P_4Ag$ 1015.3004, found 1015.2993 (55) [M–SbF_6]; calcd. for $C_{30}H_{32}P_2Ag$ 561.1030, found 561.1012 (100) [M–ligand–SbF_6]. **IR:** (KBr disc, cm^{-1}) ν = 3033w (ν_{Ar-H}), 2958m (ν_{C-H}), 1560s, 1435s, 1310s, 692s, 657vs, 540vs.

[$LCoCl_2$]: A yellow solution of **L** (300 mg, 0.66 mmol) in dichloromethane (10 mL) was added dropwise over 2 minutes to a pink solution of cobalt(II) chloride hexahydrate (157 mg, 0.66 mmol) in methanol (5 mL). During addition, the solution turned an intense green colour. The solution was left to stir for 2 hours before the volatiles were removed *in vacuo* to afford **[$LCoCl_2$]** as a mildly air-sensitive green solid (367 mg, 95%) (Mp. 257 °C decomp.). Crystals of suitable quality for X-ray diffraction were grown from slow evaporation of a solution of the complex in dry dichloromethane at ambient conditions. **Elemental Analysis:** Calcd. (%) for $C_{30}H_{32}P_2CoCl_2 \cdot CHCl_3$ (703.74): C 52.91, H 4.73; Found: C 53.03, H 5.04. **HRMS (ASAP+):** m/z (%) calcd. for $C_{30}H_{32}P_2CoCl$ 548.1000, found 548.1013 (100) [M–Cl]; m/z (%) calcd. for $C_{30}H_{33}P_2O$ 471.2007, found 471.2008 (100) [M–$CoCl_2$+OH]; calcd. for $C_{30}H_{33}P_2$ 455.2057, found 455.2059 (90) [M–$CoCl_2$+H]. **UV-Vis:** λ_{MAX} (CH_2Cl_2)/nm 701 (ε/$M^{-1}cm^{-1}$ 592), 650 (409) and 590sh (559). **IR:** (KBr disc, cm^{-1}) ν = 3048w (ν_{Ar-H}), 2981m (ν_{C-H}), 1607vs, 1436vs, 850s, 744s, 693s, 508s.

[$L^{O}CoCl_2$]: [$LCoCl_2$] (100 mg, 0.17 mmol) was dissolved in HPLC grade acetonitrile in air. The solution was swirled for 2 minutes, during which the colour of the solution changed from green to an intense blue. Removal of the volatiles *in vacuo* yielded a blue solid in a quantitative yield (102 mg, quant.). Independently, an NMR sample (in $CDCl_3$), and two crystallization attempts (solutions in MeCN and CH_2Cl_2) of green **[$LCoCl_2$]** were prepared in air. In all three cases, after 2–3 days exposure to air, blue crystalline **[$L^{O}CoCl_2$]** was isolated as the sole product (Mp. 242 °C decomp.). Crystals of suitable quality for X-ray diffraction were grown from slow evaporation of solution of the complex in acetonitrile at ambient conditions**. Elemental Analysis:** Calcd. (%) for $C_{30}H_{32}P_2CoOCl_2$·MeCN: (641.41) C 59.92, H 5.50, N 2.18; Found: C 59.82, H 5.45, N 2.24. **HRMS (ASAP+):** m/z (%) calcd. for $C_{30}H_{32}P_2OCoCl_2$ 599.0637, found 599.0634 (<1) [M+]; m/z (%) calcd. for $C_{30}H_{32}P_2CoOCl$ 564.0949, found 564.0950 (50) [M–Cl]; calcd. for $C_{30}H_{33}P_2O$ 471.2007, found 471.2003 (100) [M–$CoCl_2$+H]. **UV-Vis:** λ_{MAX} (CH_2Cl_2)/nm 680 (ε/$M^{-1}cm^{-1}$ 407), 649 (363) and 576sh (225). **IR:** (KBr disc, cm^{-1}) ν = 3051w (ν_{Ar-H}), 2929m (ν_{C-H}), 1655s, 1400vs, 1136vs ($\nu_{P=O}$), 696s, 583m.

L^{O}: Blue solid **[$L^{O}CoCl_2$]** (40 mg, 33 µmol) was dissolved in methanol (2 mL). The solution turned pink immediately. The solution was left to stand for 24 hours after which colourless crystals of **L^{O}** were collected *via* filtration and dried *in vacuo* (27 mg, 87%). The crystals that were isolated were of suitable quality for X-ray diffraction. **Elemental Analysis:** Calcd. (%) for $C_{30}H_{32}P_2O_2$·MeOH (502.56): C 74.08, H 7.22; Found: C 73.69, H 7.04. **^{1}H NMR:** δ_H (500.1 MHz, CD_2Cl_2) 7.76 (1H, dd, $^{3}J_{HH}$ = 7.2, $^{3}J_{HP}$ = 2.2 Hz, H-2), 7.64–7.58 (4H, m, H-17), 7.49–7.44 (4H, m, H-3,8,19), 7.43–7.38 (4H, m, H-18), 7.15 (1H, dd, $^{3}J_{HH}$ = 7.3, $^{4}J_{HP}$ = 1.0 Hz, H-7), 3.49–3.39 (4H, m, H-11,12), 1.94 (2H, dh, $^{3}J_{HH}$ = 6.9, $^{2}J_{HP}$ = 3.1 Hz, H-13), 0.97 (6H, dd, $^{3}J_{HP}$ = 14.1, $^{3}J_{HH}$ = 6.9 Hz, 2 × CH_3, H-14), 0.59 (6H, dd, $^{3}J_{HP}$ = 11.7, $^{3}J_{HH}$ = 6.9 Hz, 2 × CH_3, H-14). **^{13}C{^{1}H} NMR:** δ_C (125.8 MHz, CD_2Cl_2) 152.8 (s, qC-6), 148.5 (s, qC-4), 140.0 (qC-5*), 139.6 (d, $^{2}J_{CP}$ = 14.5 Hz, C-8), 139.1 (br s, qC-15), 138.3 (br s, qC-10), 136.0 (br s, C-2), 131.6 (dd, $^{2}J_{CP}$ = 8.7, $^{6TS}J_{CP}$ = 3.5 Hz, C-16), 130.1 (s, C-18), 128.0 (d, $^{3}J_{CP}$ = 12.1 Hz, C-17), 125.5 (qC-9*), 120.3 (s, C-3), 117.6 (d, $^{3}J_{CP}$ = 15.0 Hz, C-7), 30.01 (s, C-11/12), 29.97 (s, C-11/12), 26.6 (d, $^{1}J_{CP}$ = 18.7 Hz), 19.9 (d, $^{2}J_{CP}$ = 20.9 Hz, 2 × CH_3, H-14), 19.6 (d, $^{2}J_{CP}$ = 11.8 Hz, 2 × CH_3, H-15). **^{31}P{^{1}H} NMR:** δ_P (202.5 MHz, CD_2Cl_2) 32.7 (d, $^{4TS}J_{PP}$ = 6.0 Hz, P_B), –7.2 (d, $^{4TS}J_{PP}$ = 6.0 Hz, P_A). **HRMS (ASAP+):** m/z (%) calcd. for $C_{30}H_{32}P_2OH$ 471.2007, found 471.2005 (100) [M+H]. **IR:** (KBr disc, cm^{-1}) ν = 3024w (ν_{Ar-H}), 2962m (ν_{C-H}), 1587s, 1420vs, 1166vs, 731s, 692s, 556s.

L^{O2}: A yellow solution of **L** (1.00 g, 2.2 mmol) in dichloromethane (15 mL) was prepared and stirred under nitrogen. To this, hydrogen peroxide (30% aqueous solution, 3 mL) was added dropwise over 5 minutes. The solution gradually turned colourless during addition. The solution was left to stir for 2

hours. The mixture was transferred into a separating funnel and the lower organic layer collected, dried over magnesium sulfate and filtered. The volatiles were removed *in vacuo* to give $\mathbf{L^{O2}}$ as a white microcrystalline air-stable solid (1.05 g, 98%) (Mp. 175 °C decomp.). Crystals of suitable quality for X-ray diffraction were grown from slow evaporation of solution of the complex in dichloromethane at ambient conditions. **^{1}H NMR:** δ_H (500.1 MHz, CD_2Cl_2) 7.63 (1H, dd, $^3J_{HP}$ = 17.5, $^3J_{HH}$ = 7.3 Hz, H-2), 7.52 (1H, d, $^3J_{HH}$ = 7.2 Hz, H-7), 7.50–7.43 (5H, m, H-8, 17), 7.42–7.37 (6H, m, H-18, 19), 7.27 (1H, d, $^3J_{HH}$ = 7.3 Hz, H-3), 3.52–3.43 (4H, m, H-11,12), 3.01 (2H, br s, H-13), 1.26 (6H, dd, $^3J_{HP}$ = 15.4, $^3J_{HH}$ = 7.1 Hz, 2 × CH_3, H-14), 0.72 (6H, br s, 2 × CH_3, H-14). **^{13}C{^{1}H} NMR:** δ_C (125.8 MHz, CD_2Cl_2) 152.7 (qC, C-4*), 151.5 (s, qC-6), 140.7 (d, $^2J_{CP}$ = 14.4 Hz, C-2), 139.9 (dd, ~t, $^3J_{CP(A)} \approx {}^3J_{CP(B)}$ = 9.8 Hz, qC-5), 137.8 (qC-15*), 133.7 (dd, $^2J_{CP}$ = 7.3, $^2J_{CP}$ = 7.2 Hz, qC-10), 131.3 (d, $^2J_{CP}$ = 9.0 Hz, C-16), 130.5 (br s, C-8), 128.0 (s, C-18), 127.9 (s, C-17), 126.6 (qC-1*), 124.1 (qC-9*), 119.4 (br s, C-7), 118.4 (d, $^3J_{CP}$ = 15.2 Hz, C-3), 30.1 (s, C-11/12), 30.0 (s, C-11/12), 28.4 (d, $^1J_{CP}$ = 65.9 Hz, C-13), 16.5 (s, 2 × CH_3, C-14), 16.3 (d, $^2J_{CP}$ = 3.2 Hz, 2 × CH_3, C-15). **^{31}P{^{1}H} NMR:** δ_P (202.5 MHz, CD_2Cl_2) 54.7 (br s, P_A), 31.4 (br s, P_B). **MS (EI+):** m/z (%) 443.2 (100) [M–*i*Pr], 409.2 (50) [M–Ph]. **IR:** (KBr disc, cm^{-1}) ν = 3042w (ν_{Ar-H}), 2981m (ν_{C-H}), 1604s, 1437vs, 1195vs, 731s, 693s, 535s.

[$\mathbf{L^{O2}CoCl_2}$]: A colourless solution of $\mathbf{L^{O2}}$ (150 mg, 0.31 mmol) in dichloromethane (8 mL) was prepared in air. To this a pink solution of cobalt chloride hexahydrate (73 mg, 0.31 mmol) in methanol (4 mL) was added. The solution immediately turned intense blue during addition. The solution was left to stir overnight. Removal of the volatiles *in vacuo* gave **[$\mathbf{L^{O2}CoCl_2}$]** as a blue air-stable solid (188 mg, quant.) (Mp. 167 °C decomp.). Crystals of suitable quality for X-ray diffraction were grown from slow evaporation of solution of the complex in acetonitrile at ambient conditions. **Elemental Analysis:** Calcd. (%) for $C_{30}H_{32}P_2O_2CoCl_2{\cdot}CH_2Cl_2$ (701.29): C 53.09, H 4.89; Found: C 52.45, H 4.54. **HRMS (ASAP+):** m/z (%) calcd. for $C_{30}H_{32}P_2O_2CoCl$ 580.0898, found 580.0899 (5) [M–Cl]; m/z calcd. for $C_{30}H_{33}P_2O_2$ 487.1986, found 487.2007 (100) [M+H–$CoCl_2$]. **IR:** (KBr disc, cm^{-1}) ν = 3032w (ν_{Ar-H}), 2932m (ν_{C-H}), 1598s, 1438vs, 1151vs, 719s, 700s, 558s.

[$\mathbf{L^{O2}CuCl_2}$]: A colourless solution of $\mathbf{L^{O2}}$ (150 mg, 0.31 mmol) in dichloromethane (8 mL) was prepared in air. To this a blue solution of copper(II) chloride dihydrate (53 mg, 0.31 mmol) in methanol (6 mL) was added. The solution immediately turned green during addition and was left to stir overnight. Removal of the volatiles *in vacuo* gave an air-stable green solid (190 mg, quant.) (Mp. 94 °C decomp.). Crystals of suitable quality for X-ray diffraction were grown from slow evaporation of solution of the complex in toluene at ambient conditions**. IR:** (KBr disc, cm^{-1}) ν = 3053w (ν_{Ar-H}), 2930m (ν_{C-H}), 1599s, 1438vs, 1145vs, 718s, 697s, 557s.

$^{31}P\{^{1}H\}$ NMR spectra

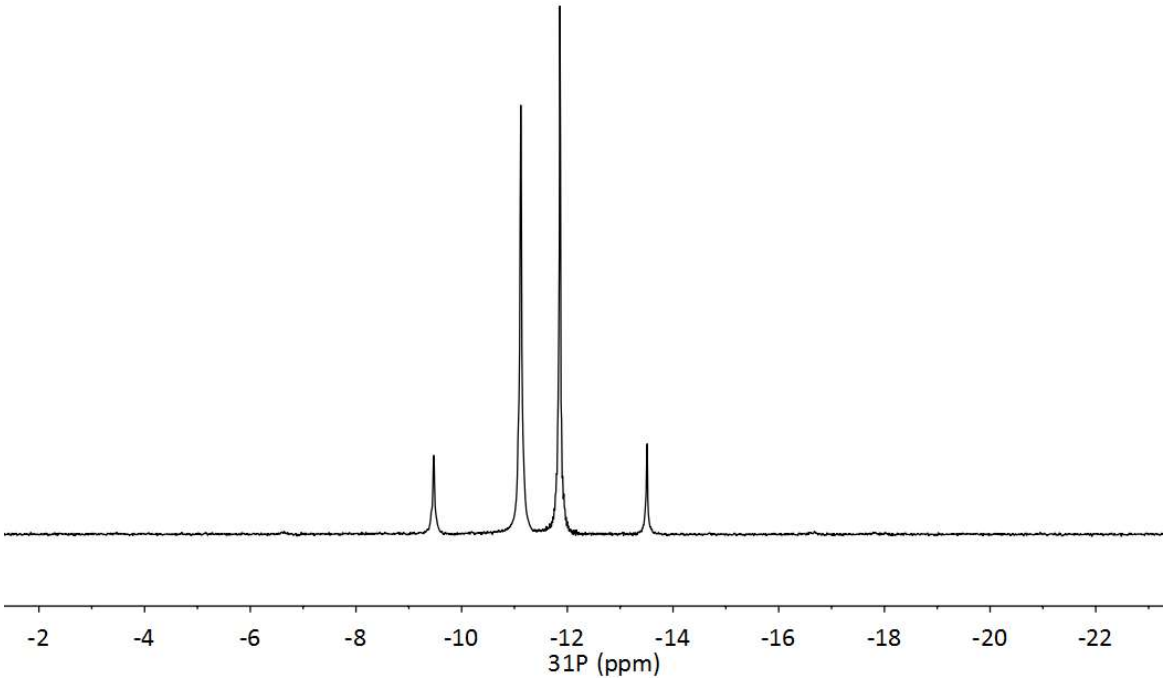

Figure S2: $^{31}P\{^{1}H\}$ NMR spectrum of **L**.

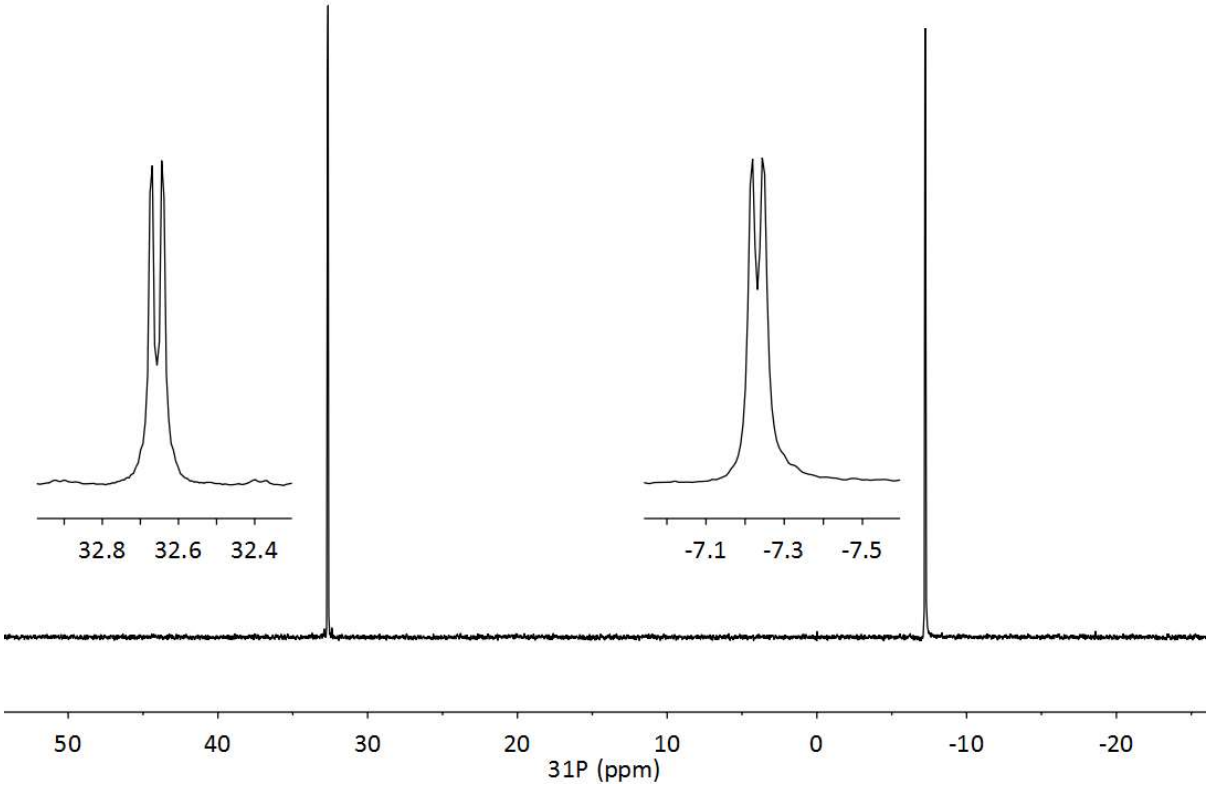

Figure S3: $^{31}P\{^{1}H\}$ NMR spectrum of $\mathbf{L^{O}}$ with expansions of each doublet showing J_{PP}.

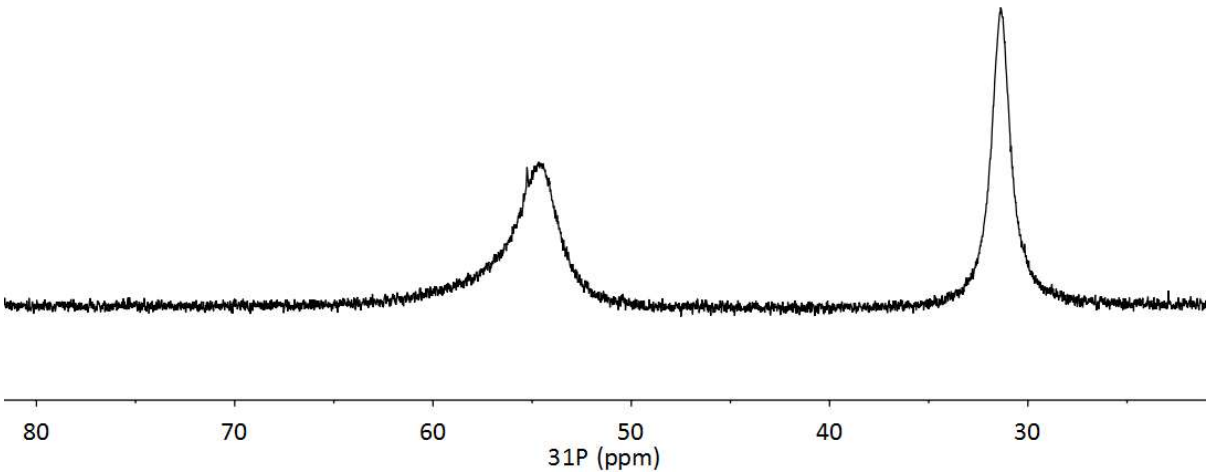

Figure S4: $^{31}P\{^{1}H\}$ NMR spectrum of $\mathbf{L^{O2}}$.

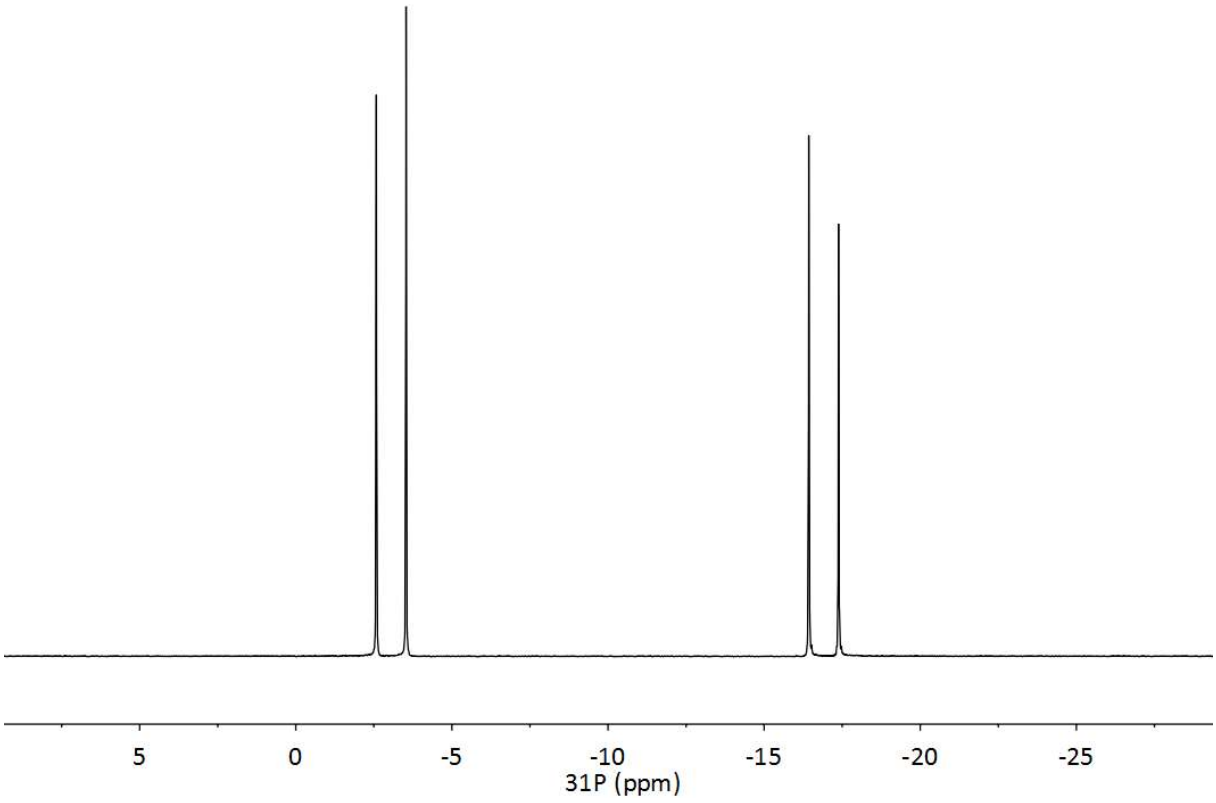

Figure S5: $^{31}P\{^{1}H\}$ NMR spectrum of **[LZnCl$_2$]**.

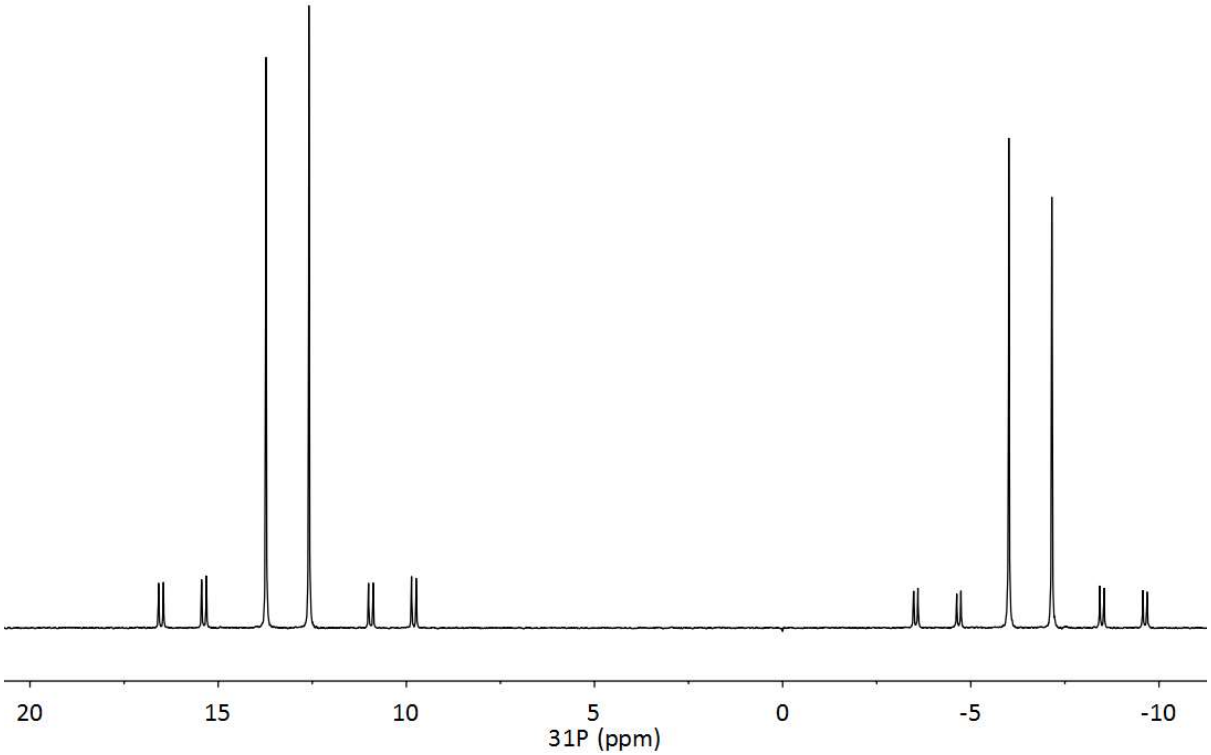

Figure S6: $^{31}P\{^{1}H\}$ NMR spectrum of **[$LCdCl_2$]**.

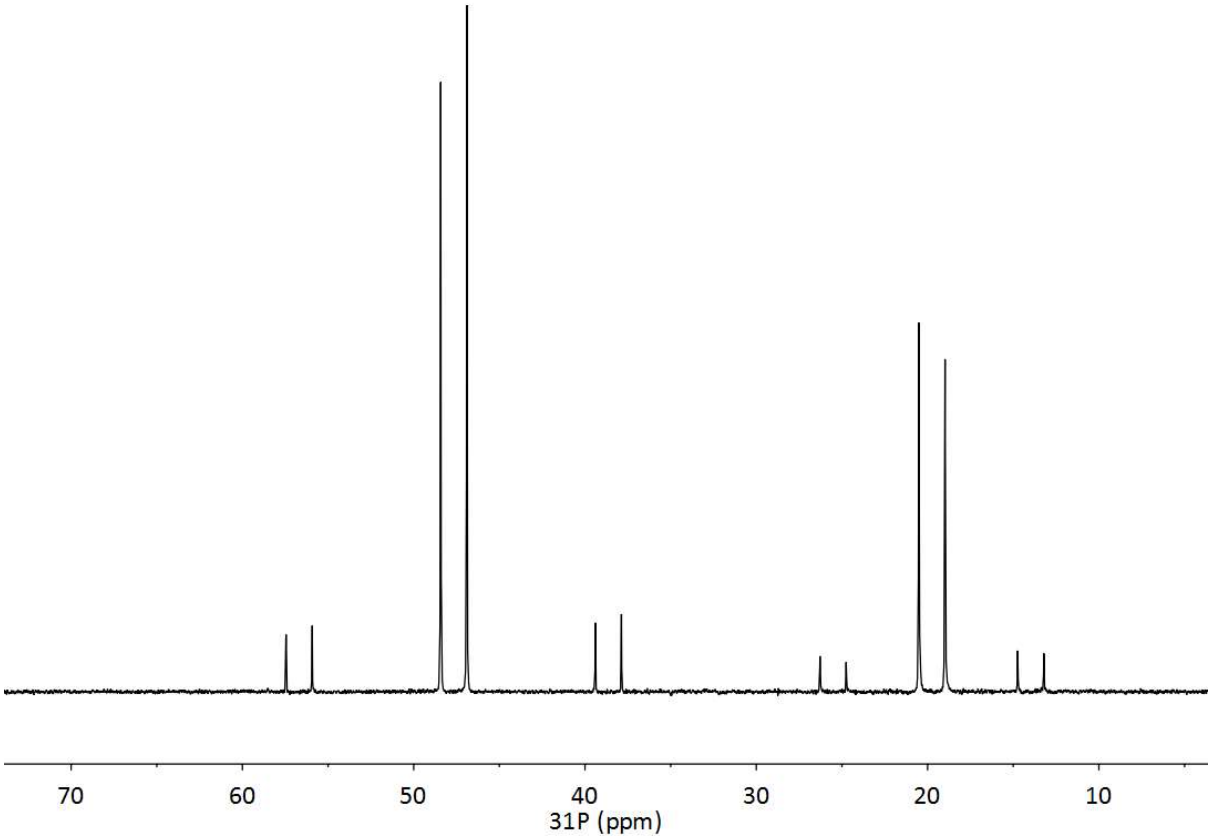

Figure S7: $^{31}P\{^{1}H\}$ NMR spectrum of **[$LHgCl_2$]**.

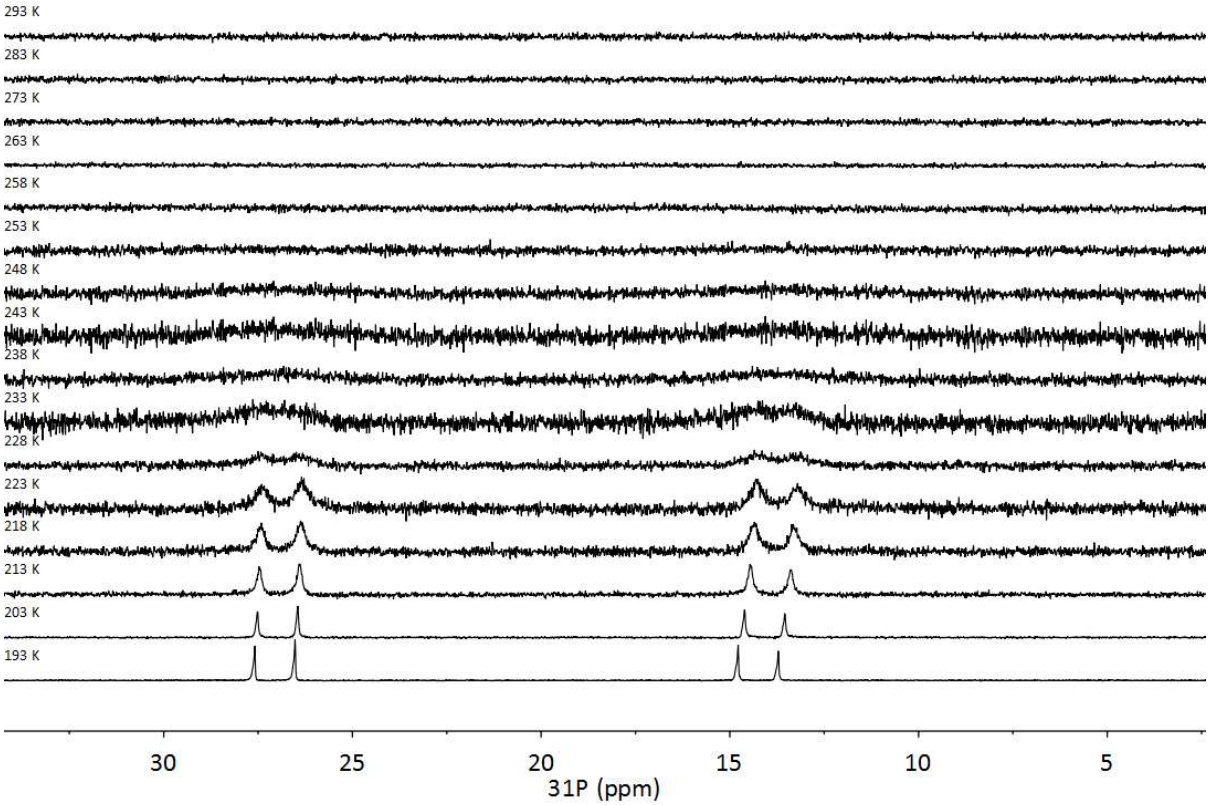

Figure S8: Full $^{31}P\{^{1}H\}$ VT NMR of **[LNiCl$_2$]** in CD_2Cl_2 recorded at 109.4 MHz.

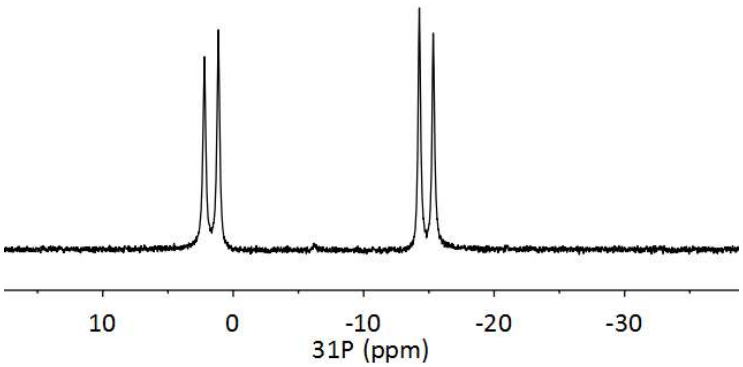

Figure S9: The $^{31}P\{^{1}H\}$ NMR spectrum of **[(LCuCl)$_2$]** acquired at 202.5 MHz.

Structural Investigations - Additional Information

The ligands (L, L^{O} and L^{O2})

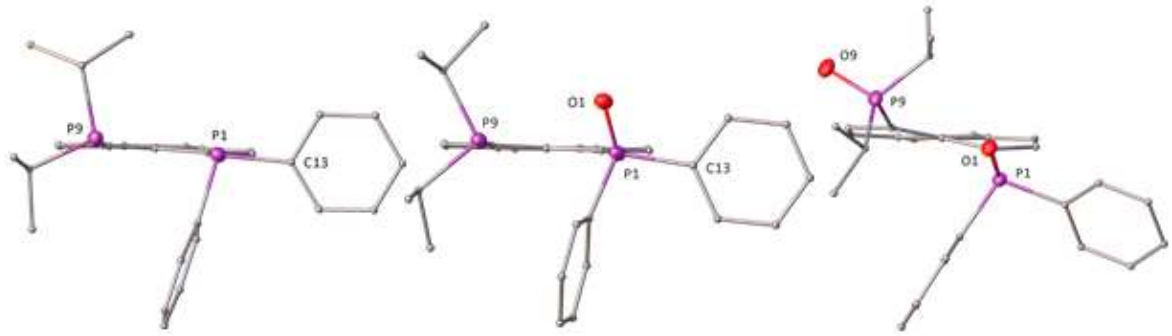

Figure S10: A view along the acenaphthene plane of **L**, $\mathbf{L^{O}}$ and $\mathbf{L^{O2}}$ to illustrate the differences in the peri-region geometry. Hydrogen atoms and solvating molecules are omitted. Thermal ellipsoids (non-carbon atoms only) are plotted at the 40 % probability level.

Group 12 and 10 [LMX_2] Complexes (M = Zn, Cd, Hg, Ni, Pd, Pt, X = Cl, Br)

As mentioned in the NMR section, the J_{PCd} and J_{PHg} couplings are directly linked to the σ-donor strength of the phosphine, with the more basic phosphine ($_{i}Pr_2P$) having a larger coupling to the metal centre (Table 1). Interestingly, this is not mirrored in the crystal structures, in which some *i*Pr_2P groups display slightly shorter P–M bond lengths than Ph_2P group, but others show the opposite.

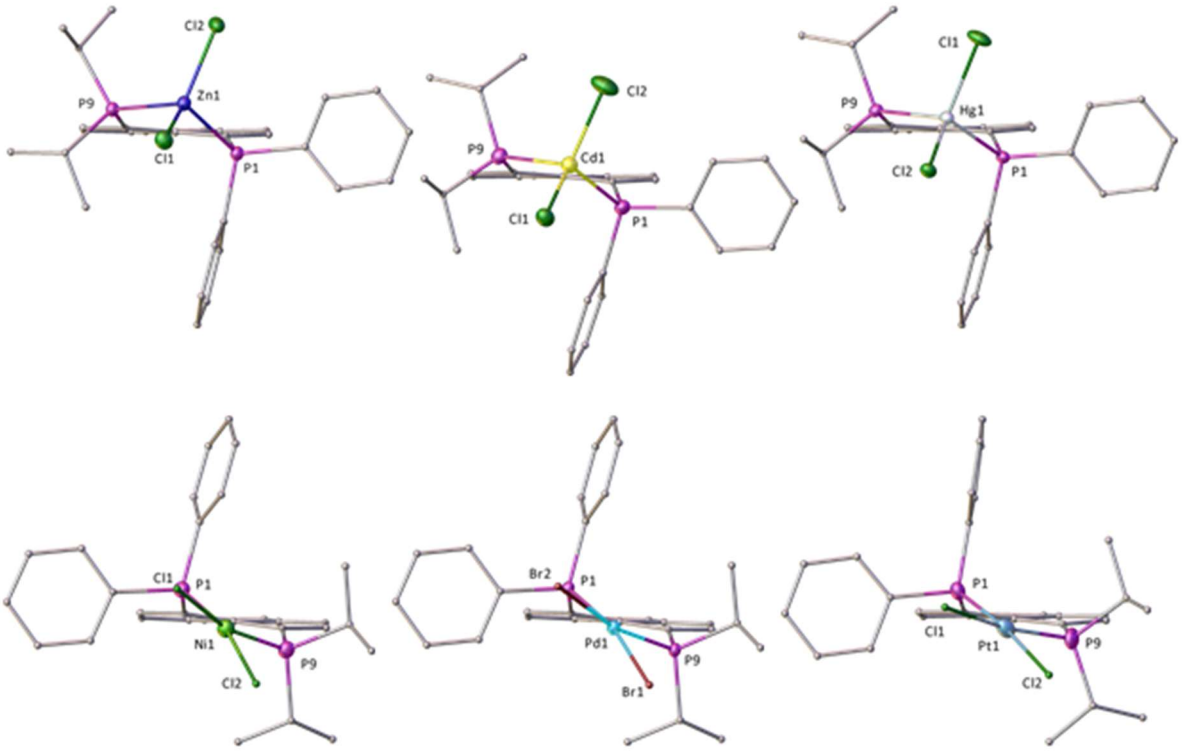

Figure S11: A view of the group 12 and 10 **[LMX$_2$]** complexes along the acenaphthene plane, highlighting the metal geometry and the peri-region geometry. Hydrogen atoms and solvating molecules are omitted. Non-carbon atoms plotted with thermal ellipsoids at the 40 % probability level.

In addition to the rather pronounced out-of-plane distortions of the ligand, the metal centres show deviations from the ideal square planar geometry. This is of interest especially for the nickel complex, as unusual magnetic properties were observed for this complex in the solution NMR (see above). The P1–Ni1–P9 *cis*-angle is 92.99(2)°. A distinct tetrahedral distortion is observable with the *trans* bond angles of 165.54(2) (P1-Ni1-Cl2) and 164.95(2) (P9-Ni1-Cl1), with similar values for Pd and Pt complexes (167.45(3) to 173.2(1)°). Although these deviations are significant, they are not sufficiently pronounced for the structures to be considered as intermediate between tetrahedral and square planar, such as seen, for example, in $CuCl_4^{2-}$ anion, where trans angles of *ca.* 135-138° have been observed.[4]

For the group 10 series, the Ph_2P–M bond lengths are slightly shorter than the *i*Pr_2P–M bond lengths, correlating with an increase in π back-bonding. In **[LPtCl$_2$]** the shorter P-Pt bond results in larger magnitude of J_{PPt} coupling. This indicates the coupling is not proportional only to the strength of the σ-component of the metal-phosphorus bond, but rather to the overall strength of the bonding (i.e. the product of σ and π interaction).

Group 11 Complexes $[(LCuCl)_2]$, $[L_2Ag]SbF_6$ and $[L^{O2}CuCl_2]$

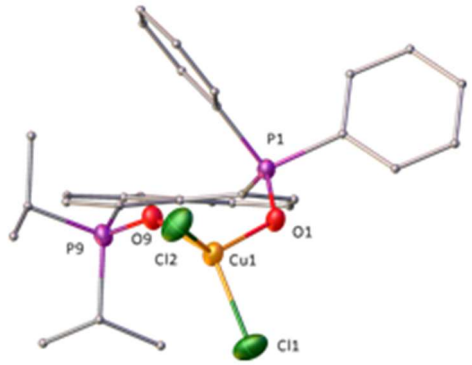

Figure S12: View of the crystal structure of **$[L^{O2}CuCl_2]$** along the acenaphthene plane, highlighting the metal and the peri-region geometry. Carbon atoms are drawn in wireframe for clarity. Solvating toluene, the second molecule in the asymmetric unit and hydrogen atoms are omitted for clarity. Thermal ellipsoids are plotted at the 40 % probability level.

Cobalt Dichloride Complexes $[LCoCl_2]$, $[L^{O}CoCl_2]$ and $[L^{O2}CoCl_2]$

Overall, there is an interesting discrepancy in *peri*-strain escalation within free ligands and Co(II) complexes series. Thus in the series of free ligands a major increase in peri-region strain occurs on transition from **L** and **L^{O}** to dioxidised ligand **L^{O2}**. However, in the Co(II) series, already the monoxidation (transition from **$[LCoCl_2]$** to **$[L^{O}CoCl_2]$**) results in major upsurge of the steric strain as judged from the extent of the distortions described in the main text.

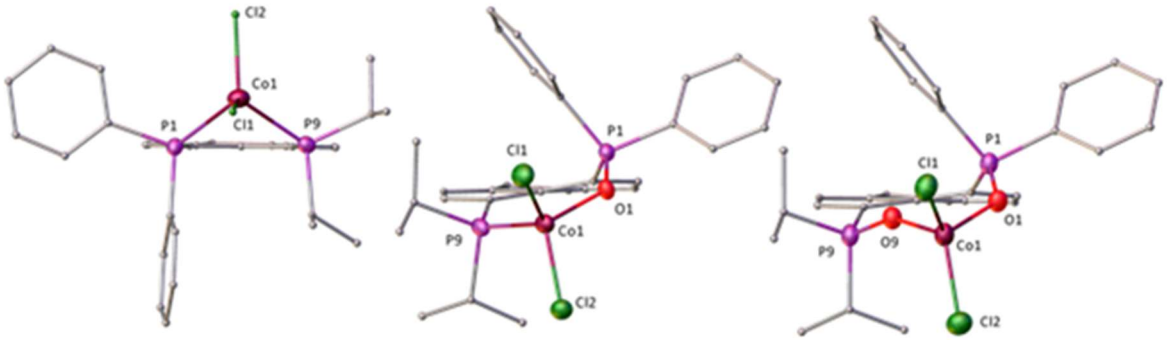

Figure S13: Views of the crystal structures of **$[LCoCl_2]$**, **$[L^{O}CoCl_2]$** and **$[L^{O2}CoCl_2]$** along the acenaphthene plane, illustrating the peri-region and metal geometry. Solvating molecules and hydrogen atoms are omitted for clarity. Non-carbon atoms are plotted as thermal ellipsoids at the 40 % probability level.

The images in Figure S14 are stills from a video of the aerobic oxidation of **[$LCoCl_2$]** in acetonitrile at ambient conditions (*ca*. 17 °C). The first image is taken 5 seconds after solvent addition and each subsequent image after a 10 second interval.

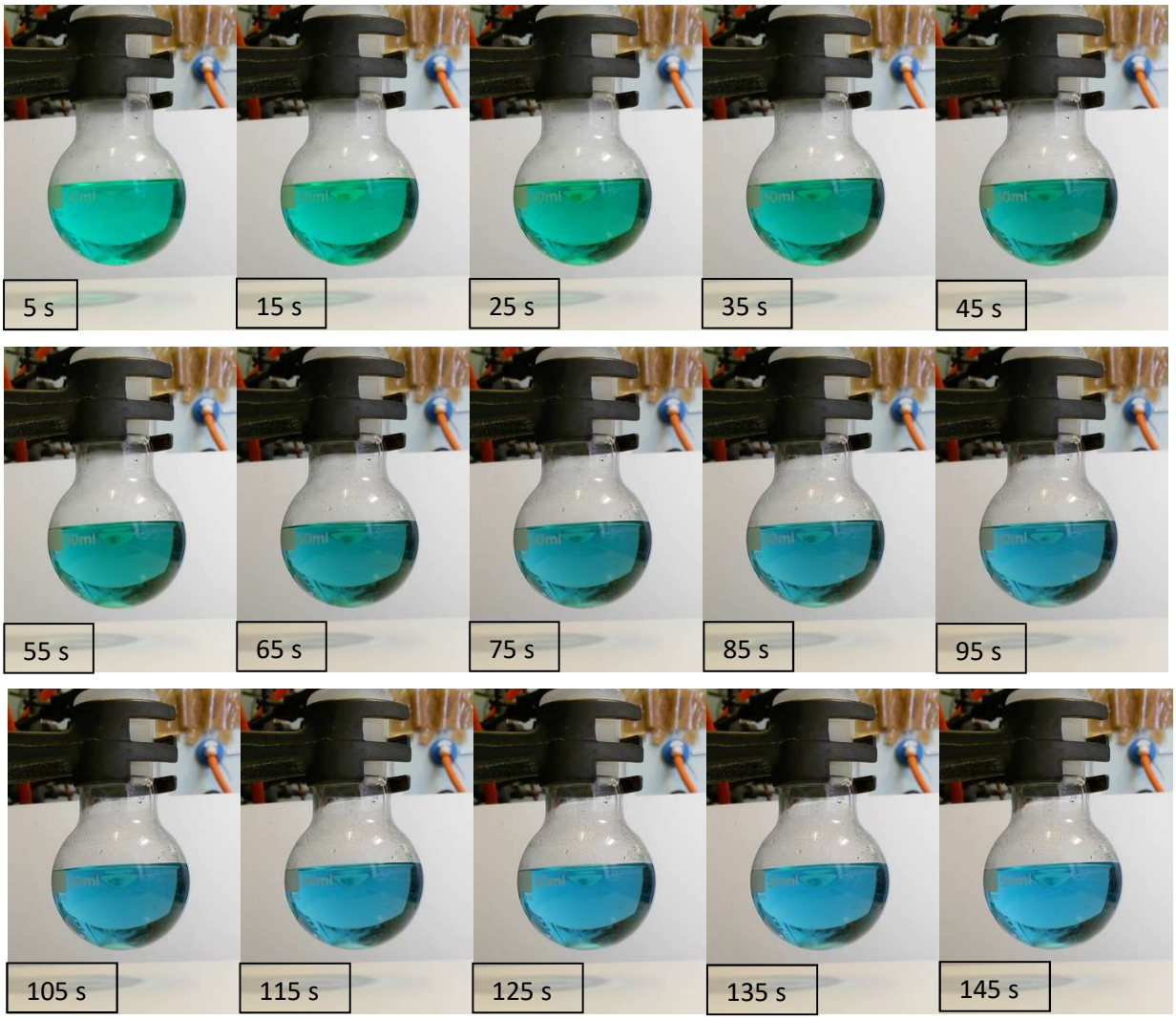

Figure S14: The oxidation of **[$LCoCl_2$]** to **[L^OCoCl_2]** in non-deoxygenated MeCN.

Figure S15: A concentrated solution of **[LCoCl$_2$]** (green) and **[L^{O}CoCl$_2$]** (blue) in deoxygenated MeCN under argon.

X-ray Diffraction

CCDC 1589108-1589120 contain the supplementary crystallographic data for this paper. These data can be obtained free of charge via www.ccdc.cam.ac.uk/structures. Selected crystallographic data are presented in Tables S1-S4.

The crystallographic data for **[LCdCl$_2$]** were collected using the St Andrews Automated Robotic Diffractometer (STANDARD),[5] consisting of a Rigaku sealed-tube generator, equipped with a SHINE monochromator [Mo Kα radiation (λ = 0.71075 Å)], and a Saturn 724 CCD area detector, coupled with a Microglide goniometer head and an ACTOR SM robotic sample changer, at –148 °C (±1). All other data were collected using a Rigaku FR-X Ultrahigh Brilliance Microfocus RA generator/confocal optics with XtaLAB P200 system, with multi-layer mirror monochromated Mo-Kα radiation at either –100 °C or –180 °C (±1) (Mo-Kα = λ = 0.71073 Å). All intensity data were collected using ω steps accumulating area detector frames spanning at least a hemisphere of reciprocal space, and were corrected for Lorentz, polarisation and long-term intensity fluctuations. Absorption effects were corrected on the basis of multiple equivalent reflections using CrystalClear.[6] Non-hydrogen atoms were refined anisotropically and hydrogen atoms were refined using a riding model. The crystal structures of **L^{O}** and **[LPdBr$_2$]** were solved using heavy–atom Patterson methods (PATTY).[7] The crystal structures of **[LZnCl$_2$]** and **[L^{O2}CuCl$_2$]** were solved using the charge flipping method (SUPERFLIP).[8] All others were solved using direct methods (SIR2004 and SIR2011)[9-10] and refined by full-matrix least-squares against F^2 (SHELXL-2014).[11] All calculations were performed using the *CrystalStructure* crystallographic software package.[12] Images of crystal structures were obtained using *OLEX2*.[13]

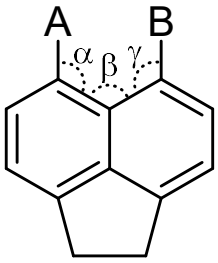

Splay angle = $\Sigma_{\alpha\beta\gamma} - 360$

Figure S16: Definition of the splay angle.

Table S1: Crystal and structure refinement data.

	L^{O}·MeOH	L^{O2}·CH_2Cl_2	**[$LZnCl_2$]**·½CH_2Cl_2	**[$LCdCl_2$]**
Formula	$C_{31}H_{36}O_2P_2$	$C_{31}H_{34}Cl_2O_2P_2$	$C_{30.5}H_{33}Cl_3P_2Zn$	$C_{30}H_{32}CdCl_2P_2$
Mr	502.57	571.46	633.28	637.85
Colour/Habit	Colourless/prism	Colourless/prism	Colourless/prism	Colourless/prism
Crystal Dimensions [mm]	0.10×0.03×0.02	0.10×0.03×0.03	0.20×0.10×0.03	0.10×0.10×0.10
Crystal System	orthorhombic	triclinic	tetragonal	monoclinic
Space Group	Pbca	P-1	$P4_32_12$	I2/a
***a* [Å]**	20.871(3)	9.886(3)	10.9286(15)	18.986(12)
***b* [Å]**	16.225(2)	11.928(3)	=*a*	17.617(9)
***c* [Å]**	15.725(2)	13.844(3)	49.588(8)	19.097(9)
α [°]	90	103.720(3)	90	90
β [°]	90	108.635(4)	90	116.56(5)
γ [°]	90	103.801(2)	90	90
V [Å^3]	5325.0(12)	1412.4(6)	5918.9(15)	5714(6)
Z	8	2	8	8
$\rho_{calcd.}$ [g cm^{-3}]	1.254	1.344	1.421	1.483
μ [cm^{-1}]	1.898	3.704	12.278	10.819
$2\theta_{max}$	50.9	50.7	50.5	50.8
F_{000}	2144.00	600.00	2616.00	2592.00
Measured refln.	28718	19511	31000	37221
Unique refln.	4922	5136	5352	5200
R [I>2σ(I)]	0.0531	0.0707	0.0237	0.0345
wR_2	0.1541	0.2293	0.0555	0.0805
Goodness of Fit	1.023	1.071	1.080	1.025
Largest peak/hole [e Å^{-3}]	0.41/–0.53	1.33/–1.06	0.28/–0.23	0.62/–0.37

Table S2: Crystal and structure refinement data.

	[$LHgCl_2$]	**[$LNiCl_2$]**·CH_2Cl_2	**[$LPdBr_2$]**·CH_2Cl_2	**[$LCoCl_2$]**
Formula	$C_{30}H_{32}Cl_2HgP_2$	$C_{31}H_{34}Cl_4NiP_2$	$C_{31}H_{34}Br_2Cl_2P_2Pd$	$C_{30}H_{32}Cl_2CoP_2$
Mr	726.03	669.07	805.67	584.37
Colour/Habit	Colourless/prism	Red/prism	Yellow/prism	Turquoise/chip
Crystal Dimensions [mm]	0.10×0.10×0.05	0.17×0.15×0.04	0.19×0.09×0.03	0.08×0.04×0.01
Crystal System	monoclinic	monoclinic	monoclinic	monoclinic
Space Group	I2/a	$P2_1/c$	$P2_1/c$	$P2_1/c$
***a* [Å]**	18.900(5)	14.7245(16)	14.7439(13)	11.430(2)
***b* [Å]**	17.557(4)	10.8016(14)	11.0535(9)	11.029(2)
***c* [Å]**	19.227(4)	18.746(3)	18.7810(16)	22.449(4)
α [°]	90	90	30	90
β [°]	117.300(18)	91.805(4)	91.974(3)	93.650(5)
γ [°]	90	90	90	90
V [Å^3]	5669(2)	2980.0(7)	3059.0(5)	2824.2(9)
Z	8	4	4	4
$\rho_{calcd.}$ [g cm^{-3}]	1.701	1.491	1.749	1.374
μ [cm^{-1}]	57.630	11.377	35.273	9.277
$2\theta_{max}$	50.9	50.8	50.8	50.7
F_{000}	2848.00	1384.00	1600.00	1212.00
Measured refln.	21663	35642	36731	33870
Unique refln.	5182	5442	5597	5153
R [I>2σ(I)]	0.0186	0.0251	0.0253	0.0717
wR_2	0.0684	0.0673	0.0697	0.1889
Goodness of Fit	1.118	1.047	1.046	1.029
Largest peak/hole [e Å^{-3}]	0.70/–1.21	0.83/–0.56	2.11/–0.82	2.43/–0.99

Table S3: Crystal and structure refinement data.

	[$L^{O}CoCl_2$]·MeCN	**[$L^{O2}CoCl_2$]**·MeCN	**[$(LCuCl)_2$]**·2$CHCl_3$	**[L_2Ag]SbF_6**·MeOH
Formula	$C_{32}H_{35}Cl_2CoNOP_2$	$C_{32}H_{35}Cl_2CoNO_2P_2$	$C_{62}H_{66}Cl_8Cu_2P_4$	$C_{61}H_{68}AgF_6OP_4Sb$
Mr	641.42	657.42	1345.81	1284.71
Colour/Habit	Blue/prism	Blue/prism	Yellow/prism	Yellow/prism
Crystal Dimensions [mm]	0.12×0.02×0.02	0.12×0.10×0.02	0.12×0.10×0.03	0.15×0.15×0.15
Crystal System	triclinic	triclinic	triclinic	triclinic
Space Group	P-1	P-1	P-1	P-1
***a* [Å]**	9.658(3)	9.884(3)	11.1380(14)	13.529(2)
***b* [Å]**	10.646(3)	10.808(4)	12.8894(11)	13.8435(16)
***c* [Å]**	16.134(4)	16.336(6)	13.1341(19)	16.8605(17)
α [°]	103.426(4)	103.838(7)	116.640(7)	66.873(9)
β [°]	96.059(4)	95.282(5)	98.541(16)	79.430(9)
γ [°]	107.328(6)	107.605(5)	100.376(12)	82.5909(10)
V [Å^3]	1512.8(7)	1589.4(10)	1600.5(4)	2849.1(6)
Z	2	2	1	2
$\rho_{calcd.}$ [g cm^{-3}]	1.408	1.374	1.396	1.497
μ [cm^{-1}]	8.761	8.380	11.353	9.884
$2\theta_{max}$	50.7	50.5	50.7	50.7
F_{000}	666.00	682.00	692.00	1308.00
Measured refln.	20606	19332	17832	35957
Unique refln.	5532	5615	5832	10305
R [I>2σ(I)]	0.0758	0.0798	0.0674	0.0581
wR_2	0.2155	0.2301	0.1878	0.1361
Goodness of Fit	1.065	1.045	1.111	1.035
Largest peak/hole [e Å^{-3}]	2.11/–0.54	0.94/–0.71	0.78/–0.97	1.26/–0.99

Table S4: Crystal and structure refinement data.

	[$L^{O2}CuCl_2$]·½C_7H_8
Formula	$C_{33.5}H_{36}Cl_2CuO_2P_2$
Mr	667.05
Colour/Habit	Yellow/prism
Crystal Dimensions [mm]	0.20×0.17×0.04
Crystal System	monoclinic
Space Group	$P2_1$
***a* [Å]**	16.6509(12)
***b* [Å]**	9.6316(5)
***c* [Å]**	20.6837(16)
α [°]	90
β [°]	108.2170(18)
γ [°]	90
V [Å^3]	3150.9(4)
Z	4
$\rho_{calcd.}$ [g cm^{-3}]	1.406
μ [cm^{-1}]	9.936
$2\theta_{max}$	50.8
F_{000}	1384.00
Measured refln.	39119
Unique refln.	11336
R [I>2σ(I)]	0.0295
wR_2	0.0756
Goodness of Fit	1.023
Largest peak/hole [e Å^{-3}]	0.55/–0.40

Computational Details

Starting from XRD-refined coordinates, structures were fully optimised at the RI-BP86-D3(BJ)/Wachters/6-31G* level[14-18] (a level that performs well for metal-ligand bond distances in transition metal complexes), and spin-spin coupling constants were computed at the B3LYP/Wachters/IGLO-II" level.[19-20] Wachters bases used on the metals were augmented with two diffuse p and one diffuse d function (contraction scheme 62111111/3311111/3111),[21-22] and IGLO-II" basis is based on the basis sets developed for magnetic properties in the Kutzelnigg group using an uncontracted 11s7p2d basis on P, contracted 7s6p2d and 5s4p1d bases on Cl and C, respectively, and a double zeta (2s) basis on H. W. Kutzelnigg, U. Fleischer, M. Schindler, in: *NMR Basic Principles and Progress* [23]. Coupling pathways were visualised using the coupling deformation density (CDD)[24] computed at the PP86 level.[15-16, 25-26] For visualization a local version of the deMon-NMR program[27-28] was employed.

References

1. Armarego, W. L. F.; Chai, C. L. L., *Purification of Laboratory Chemicals (6th Edition)*. 6th ed.; Elsevier: Burlington.

2. Chalmers, B. A.; Athukorala Arachchige, K. S.; Prentis, J. K. D.; Knight, F. R.; Kilian, P.; Slawin, A. M. Z.; Woollins, J. D., Sterically Encumbered Tin and Phosphorus peri-Substituted Acenaphthenes. *Inorg. Chem.* **2014,** *53* (16), 8795-8808.

3. Zinin, V.; Il'yasov, A.; Thiele, H.; Hägele, G.; Weber, U., WIN-DAISY: Application to oriented molecules. Analysis and simulation of NEMA-NMR spectra. *Appl. Magn. Reson.* **1995,** *8* (2), 311-317.

4. Halvorson, K. E.; Patterson, C.; Willett, R. D., Structures of bis(4-aminopyridinium) tetrachlorocuprate(II) monohydrate, [C5H7N2]2[CuCl4].H2O and bis(2-amino-3-hydroxypyridinium) tetrachlorocuprate(II), [C5H7N2O]2[CuCl4]: correlation of CuCl42- geometry with hydrogen bonding and electronic structure. *Acta Crystallographica Section B* **1990,** *46* (4), 508-519.

5. Fuller, A. L.; Scott-Hayward, L. A. S.; Li, Y.; Bühl, M.; Slawin, A. M. Z.; Woollins, J. D., Automated Chemical Crystallography. *J. Am. Chem. Soc.* **2010,** *132* (16), 5799-5802.

6. *CrystalClear-SM Expert*, 2.1; Rigaku Americas and Rigaku Corporation The Woodlands, Texas, USA and Tokyo, Japan, 2015.

7. Beurskens, P. T. B., G.; de Gelder, R.; Garcia-Granda, S.; Gould, R. O.; Israel, R.; Smits, J. M. M. *DIRDIF-99*, Crystallography Laboratory, University of Nijmegen, The Netherlands, 1999.

8. Palatinus, L.; Chapuis, G., SUPERFLIP– a computer program for the solution of crystal structures by charge flipping in arbitrary dimensions. *J. Appl. Crystallogr.* **2007,** *40* (4), 786-790.

9. Burla, M. C.; Caliandro, R.; Camalli, M.; Carrozzini, B.; Cascarano, G. L.; De Caro, L.; Giacovazzo, C.; Polidori, G.; Spagna, R., SIR2004: an improved tool for crystal structure determination and refinement. *J. Appl. Crystallogr.* **2005,** *38* (2), 381-388.

10. Burla, M. C.; Caliandro, R.; Camalli, M.; Carrozzini, B.; Cascarano, G. L.; Giacovazzo, C.; Mallamo, M.; Mazzone, A.; Polidori, G.; Spagna, R., SIR2011: a new package for crystal structure determination and refinement. *J. Appl. Crystallogr.* **2012,** *45* (2), 357-361.

11. Sheldrick, G., Crystal structure refinement with SHELXL. *Acta Crystallographica Section C* **2015,** *71* (1), 3-8.

12. *CrystalStructure*, 4.2; Rigaku Americas, The Woodlands, Texas, USA, and Rigaku Corporation, Tokyo, Japan, 2015.

13. Dolomanov, O. V.; Bourhis, L. J.; Gildea, R. J.; Howard, J. A. K.; Puschmann, H., OLEX2: a complete structure solution, refinement and analysis program. *J. Appl. Crystallogr.* **2009,** *42* (2), 339-341.

14. Becke, A. D., Density-functional exchange-energy approximation with correct asymptotic behavior. *Phys. Rev. A* **1988,** *38* (6), 3098-3100.

15. Perdew, J. P., Density-functional approximation for the correlation energy of the inhomogeneous electron gas. *Phys. Rev. B* **1986,** *33* (12), 8822-8824.

16. Perdew, J. P., Erratum: Density-functional approximation for the correlation energy of the inhomogeneous electron gas. *Phys. Rev. B* **1986,** *34* (10), 7406-7406.

17. Grimme, S.; Antony, J.; Ehrlich, S.; Krieg, H., A consistent and accurate ab initio parametrization of density functional dispersion correction (DFT-D) for the 94 elements H-Pu. *J. Chem. Phys.* **2010,** *132* (15), 154104.

18. Becke, A. D.; Johnson, E. R., Exchange-hole dipole moment and the dispersion interaction. *J. Chem. Phys.* **2005,** *122* (15), 154104.

19. Becke, A. D., Density‐functional thermochemistry. III. The role of exact exchange. *J. Chem. Phys.* **1993,** *98* (7), 5648-5652.

20. Lee, C.; Yang, W.; Parr, R. G., Development of the Colle-Salvetti correlation-energy formula into a functional of the electron density. *Physical Review B* **1988,** *37* (2), 785-789.

21. Hay, P. J., Gaussian basis sets for molecular calculations. The representation of 3d orbitals in transition‐metal atoms. *J. Chem. Phys.* **1977,** *66* (10), 4377-4384.

22. Wachters, A. J. H., Gaussian Basis Set for Molecular Wavefunctions Containing Third‐Row Atoms. *J. Chem. Phys.* **1970,** *52* (3), 1033-1036.

23. Kutzelnigg, H. W.; Fleischer, U.; Schindler, M., In *NMR Basic Principles and Progress*, Springer-Verlag: Berlin, 1990; Vol. 23, p 165.

24. Malkina, O. L.; Malkin, V. G., Visualization of Nuclear Spin–Spin Coupling Pathways by Real-Space Functions. *Angew. Chem. Int. Ed.* **2003,** *42* (36), 4335-4338.

25. Perdew, J. P.; Wang, Y., *Phys. Rev. B.* **1989,** *40*, 3399.

26. Perdew, J. P.; Wang, Y., *Phys. Rev. B.* **1986,** *33*, 8800-8802.

27. Salahub, D. R.; Foumier, R.; Mlynarski, P.; Papai, I.; St-Amant, A.; Ushio, J., Density Functional Methods in Chemistry. In *Density Functional Methods in Chemistry*, Labanowski, J. K.; Andzelm, J. W., Eds. Springer: Berline, 1991; p 77.

28. V. G. Malkin, O. L. M., deMon-NMR program, version 2016.